Fluorescence of Dyes Adsorbed on Highly Organized, Nanostructured Gold Surfaces

Stefano A. Levi,[a, c] Ahmed Mourran,[b] Joachim P. Spatz,[b, d] Frank C. J. M. van Veggel,[a] David N. Reinhoudt,*[a] and Martin Möller*[b]

Abstract: It is shown that fluorescent dyes can be adsorbed selectively on gold nanoparticles which are immobilized on a glass substrate and that the fluorescence originating from the adsorbed dyes exhibits *significantly less quenching* when compared to dyes adsorbed on bulk gold. Self-assembled monolayers of lissamine sulfide molecules have been studied both on bulk gold and on glass surfaces bearing gold nanoparticles. Gold nanoparticles have been arranged in ordered, two-dimensional patterns, with periodicity in the μm range and used as substrate for the fluorescent dyes. Optical resolution of the fluorescence originating from the pattern has been achieved with laser-scanning confocal microscopy.

Keywords: fluorescence · gold · monolayers · nanostructures · spatial organization

Introduction

Important challenges in the rapidly expanding field of nanotechnology with respect to applications, such as devices for high-density data storage (HDDS)[1] and highly sensitive bioanalytical methods, for example, lab on a chip.[2] Common to both applications is the focus on low detection limits and the confinement in space to the nanometer scale. Analytical and bioanalytical methods[3] gain primarily from increasing sensitivity and selectivity of the detection methods and on simplifying the procedures by eliminating intermediate sampling steps and avoiding the use of radioactive probes or other types of hazardous reagents.[4, 5] Nowadays, the detection limits are pushed to the single-molecule scale. Single-molecule spectroscopy can probe organic and biomolecules and provide information on their structure and function that is difficult and sometimes impossible to obtain by conventional techniques.[6–8] High-density data storage methods focus on addressing materials at the nanometer level and therefore also deal with very low detection limits.[9] Moreover, the engineering of HDDS systems requires the nanometer confinement of functional units in space. Research is therefore pushed to observe, address, and ultimately manipulate individual molecules. Three fundamental requirements are necessary to achieve this: 1) the presence of an addressable function at a molecular level (e.g., optically switchable systems based on fluorescence);[10–13] 2) immobilization of suitable molecules on a surface (e.g., by self-assembly processes);[14] and 3) confinement of this function in a two- or three-dimensional matrix (e.g., by patterning with Au nanoparticles).[15, 16]

Of the diverse optically based detection methods, only few refer to fluorescence in combination with metal layers. The reason for this is due to the presence of a radiationless energy transfer (quenching of fluorescence) from the dye to the surface that arises if fluorescent dyes are placed in close proximity to metallic surfaces.[17] The quenching strongly depends on the distance between the dye molecule and the surface. For distances ≤ 50 nm from a continuous metal surface, it is known that the quenching efficiency increases with the power of six of the metal–dye distance.[17–19] However, some authors have reported fluorescence measurements of dyes directly adsorbed onto a polycrystalline gold layer,[20] but the fluorescent signal is weak and advanced detection techniques with modified geometries in the experimental setup are needed to increase the detection sensitivity.[3, 21, 22] Others have extensively studied the surface en-

[a] Prof. Dr. Ir. D. N. Reinhoudt, Dr. S. A. Levi, Dr. Ir. F. C. J. M. van Veggel
Supramolecular Chemistry and Technology Group and MESA+ Research Institute, University of Twente
P.O. Box 217, 7500 AE Enschede (The Netherlands)
Fax: (+31) 53-489-4645
E-mail: smct@ct.utwente.nl

[b] Prof. Dr. M. Möller, Dr. A. Mourran, Prof. Dr. J. P. Spatz
Macromolecular and Organic Chemistry III
University of Ulm, 89073 Ulm (Germany)

[c] Dr. S. A. Levi
Present Address: SusTech GmbH & Co. KG
Petersenstrasse 20, 64287 Darmstadt (Germany).

[d] Prof. Dr. J. P. Spatz
Present Address: Institute for Physical Chemistry
Biophysical Chemistry, Heidelberg University, INF 253
69120 Heidelberg (Germany)

  0947-6539/02/0816-3808 $ 20.00+.50/0

hanced fluorescence in combination with nanostructured metal surfaces, in particular with Ag nanoparticles.[17, 23, 24]

The use of nanostructured surfaces offers an alternative, since their electronic properties are remarkably different from the corresponding bulk materials.[25] At small sizes, (much smaller than the wavelength of light) metallic nanoparticles can be penetrated by electromagnetic waves; this induces a separation of charges and consequently a coherent oscillation (particle plasmons).[26] This results in an enhancement of the electromagnetic field and, therefore, in a different behavior of fluorescent molecules in close vicinity of the metal nanoparticles.[27] Examples of applications of this phenomenon can be found in detection methods such as surface-enhanced raman scattering (SERS), and surface-enhanced fluorescence (SEF). However, these techniques used in combination with metal nanoparticles have yet to be fully explored.[28–32]

Here, we describe fluorescence studies of a xanthene-based dye molecule that selectively binds to gold on different types of substrates. In the first part of this paper the synthesis of the fluorescent probe; its behavior on bulk gold is described and compared to the case of gold nanoparticles. In the second part the morphology of the gold was changed from continuous bulk films to 10 nm gold particles that were arranged in an ordered nanopattern by means of self-assembly of diblock-copolymers and surface-topology-controlled dewetting. The fluorescence originated from the dye molecules adsorbed on substrates with a high degree of order could be resolved by using laser-scanning confocal microscopy (LSCM).

Results and Discussion

Lissamine (rhodamine B sulfonyl chloride *p*-isomer) was chosen as the probe for the experiments described in this article because of its high quantum efficiency ($\eta = 0.99$) and its easy functionalization. Reaction of **1** with **2** in dry dichloromethane, in presence of an excess of triethylamine, gave lissamine sulfide **3**, a pink highly fluorescent solid (Scheme 1).

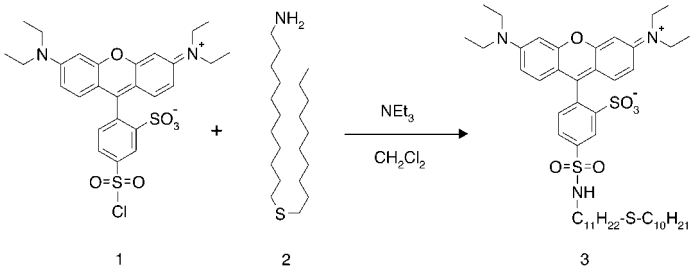

Scheme 1. Synthesis route for the preparation of lissamine sulfide adsorbate **3** from lissamine and sulfide **2**.

The sulfide functionalization accounts for a selective binding of the molecule to gold surfaces, whereas the alkyl chain (11 carbon atoms) keeps the chromophore, and, therefore, the fluorescently active part of **3** at a constant distance of ~ 2 nm from the Au substrate.

To investigate whether the fluorescence intensity of **3** bound to gold is affected by breaking up a continuous gold film into particles, the fluorescence was studied across the borderline of a 20 nm thick layer of Au that was evaporated on glass. A large area of the glass substrate was screened by a shadow mask in contact with the substrate preventing deposition of the gold only on part of the sample. At the borderline between the gold evaporated area and the bare glass, the gold film thinned before it finally broke up as shown by the scanning force microscopy image in Figure 1. A region of approximately 8 μm width was formed in which the glass substrate presents sputtered nanoparticles with diameters ranging from 2 to 5 nm.

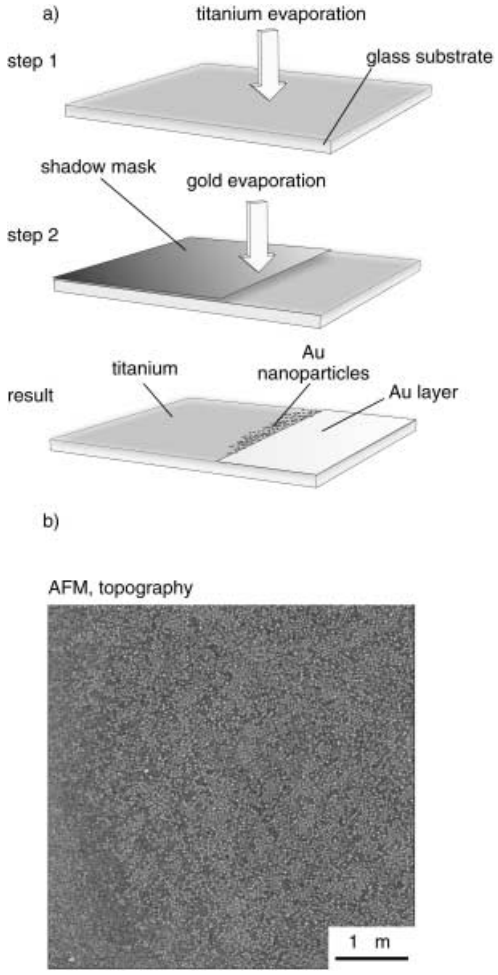

Figure 1. a) Preparation of a evaporated gold substrate by the shadow-mask technique; thickness of the homogeneous Au layer is 20 nm. b) Evaporation of Au through a shadow-mask produces a borderline with a gradient in the gold thickness and a region of ~ 5 μm, covered by gold nanoparticles with size ranging from 2 to 5 nm.

To improve the adherence of the gold to the glass, some samples were prepared with a 3 nm thick Ti layer evaporated on the whole glass substrate before deposition of the gold layer (Figure 1).

Immersion of the substrate in the lissamine sulfide solution lead to selective adsorption of **3**. LSCM images were recorded, and the intensity of fluorescence was measured across the borderline exposing gold nanoparticles (Figure 2).

  0947-6539/02/0816-3809 $ 20.00+.50/0

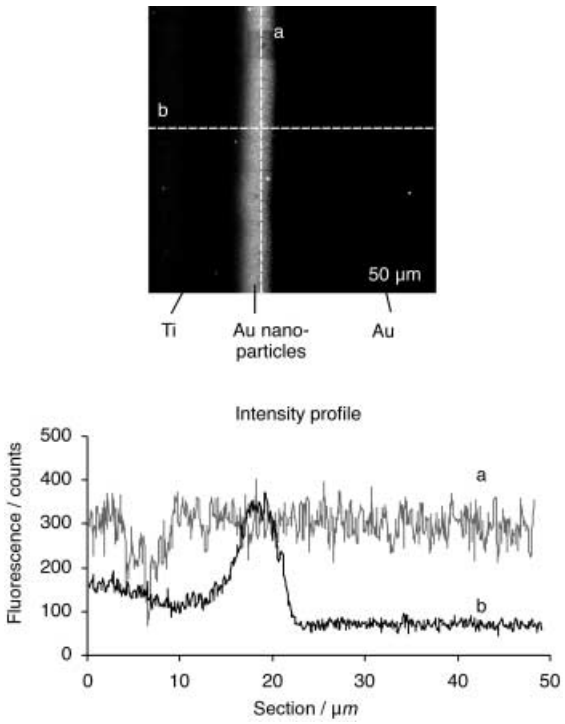

Figure 2. Top: laser scanning confocal fluorescence image of a sample exposing titanium (left area), gold nanoparticles (central area) and bulk gold (right area). The dark spot surrounded by a dark rectangular area shows the bleaching effect of the scanning laser. Bottom: fluorescence intensity cross-sections along lines a and b.

The avalanche photodiode (APD) detector did not show any fluorescence intensity for the section covered by a continuous layer of gold. This was expected because of the radiationless energy transfer to the metal. On the TiO_2-protected glass a weak fluorescence signal could be detected due to physisorption of the fluorophores on the polar surface. Most remarkable, however, was the presence of fluorescence at the borderline of the continuous gold film.

The increased fluorescence intensity at the transition zone indicates reduced fluorescence quenching of dye molecules bound to nanometer-size gold particles.

To study this phenomenon further, a glass substrate was designed bearing gold nanoparticles arranged in a highly ordered hexagonal pattern. The size and arrangement of Au nanoparticles on a flat substrate was controlled by using micelles of polystyrene-*block*-poly(2-vinylpyridine) in toluene to deposit the gold clusters. The diblockcopolymer used here consisted of 1700 styrene units linked to a block of 450 2-vinylpyridine units, PS_{1700}-*block*-$P2VP_{450}$. By treating the micelle solution with solid $HAuCl_4$, the poly(2-vinylpyridine) core was loaded with a defined number of Au ions. $AuCl_4^-$ ions are complexed to the protonated pyridine units and, therefore, are confined in the center of the micelle.[33] Addition of a reducing agent (e.g., hydrazine) yielded a single gold particle in each micelle. A monofilm of the gold-loaded micelles can be obtained by spin coating or dip coating on suitable substrate (e.g., glass, mica, and silicon). Etching with oxygen plasma allowed the removal of the polymer and yielded isolated gold nanoparticles arranged on the surface in an hexagonal pattern (Figure 3).[15, 34]

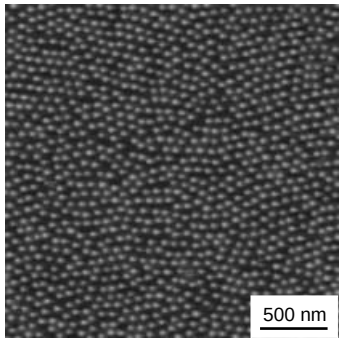

Figure 3. Tapping mode AFM image of a glass substrate decorated with 12 nm gold nanoparticles. Interparticle distance: ~80 nm.

Our major concern in this work was the ability to resolve the fluorescence that originated from molecules adsorbed on individual nanoparticles, which are fixed on a solid substrate. By using the diblock-copolymer strategy, the maximum lateral distances between nanoparticles (140–150 nm) were not resolved by confocal or standard optical microcopies. For an easy investigation by optical methods, the nanoparticles have to be separated by distances comparable with the wavelength of light employed for detection (~500 nm). To achieve separation in the µm range, Au-loaded micelles were deposited on a pre-structured substrate.[35] Meniscus forces that develop upon evaporation of the solvent at the steps in the surface structure account for the alignment of the particles in a microscopic pattern (Figure 4).

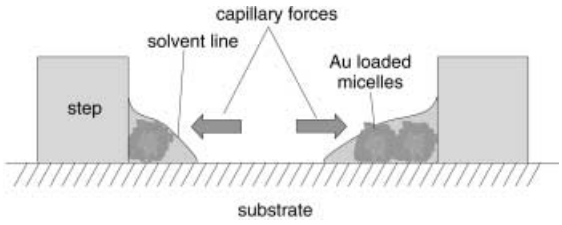

Figure 4. Positioning of block-copolymer micelles against obstacles by the action of capillary forces.

In the present study, the so-called breath-figure technique was used to pattern the substrate.[36, 37]

Thin polymer films patterned with hexagonally ordered holes were prepared simply by casting a solution of a fluoro ester derivative of polymethacrylate under a humid atmosphere onto a glass plate. Evaporation of the solvent induced condensation of small water droplets, which packed in regular order. As the solvent evaporated, the polymer vitrified and the condensation pattern was quenched. After evaporation of the water holes remained where the droplets had been. A statistical copolymer of equimolar composition of methyl methacrylate and a methacrylate derivative with a trimeric hexafluoropropyleneoxyde substituent, poly[MMA-*co*-MA($HFPO_3$)] in combination with a nonpolar, low boiling-point solvent (1,1,2-trichlorofluoroethane), ensured quick evaporation and efficient stabilization of the water droplets.

When a very dilute solution of the diblock-copolymer micelles, previously loaded with gold, was cast on such honeycomb-like substrates, the micelles were positioned

  0947-6539/02/0816-3810 $ 20.00+.50/0 *Chem. Eur. J.* **2002**, *8*, No. 16

along the walls of the template. This was caused by the effect of capillary forces in combination with the moving contact line during the evaporation of the solvent.[36, 37] Figure 5a shows a transmission electron microscopy (TEM) image of

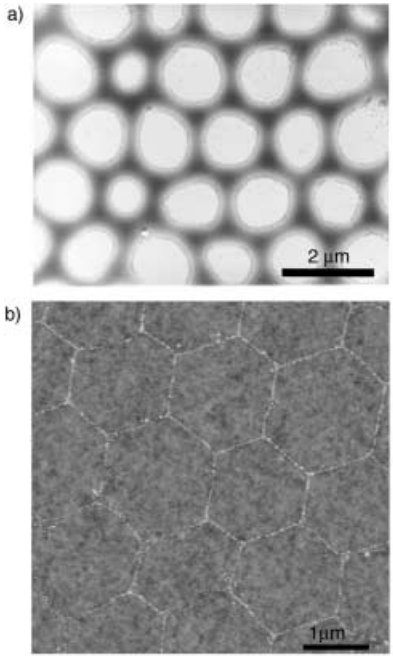

Figure 5. a) TEM image of micelles cast on a breath figure polymer template.[36] b) Tapping mode AFM image of gold nanoparticles in a honeycomb-like arrangement.

such a breath figure, which was generated on a carbon-coated TEM grid, and on which $AuCl_4^-$-loaded micelles were cast. In this particular case, a wall of 100–200 nm width separates cavities that have diameters in the micrometer range. The gold particles, still enclosed in the polymer micelle and aligned along the circular rim, can be identified clearly. From atomic force microscopy (AFM) the height of the walls was determined to be around 200 nm.

Upon plasma etching the relative position of the gold nanoparticles remains unaffected. After removal of all organic material, an AFM investigation confirmed the presence of 10 nm-size gold nanoparticles with a honeycomb-like structure arrangement (Figure 5b).

When such a substrate was treated by a solution of lissamine sulfide **3** in ethanol at 60 °C, **3** adsorbed preferentially to the Au nanoparticles. Most of the nonspecifically physisorbed material could easily be removed by rinsing with organic solvents.

Figure 6 shows a LSCM fluorescence image of a glass substrate bearing gold nanoparticles in a honeycomb-like arrangement that were functionalized with the fluorescent dye **3**. The fluorescence pattern detected clearly corresponds to the honeycomb structures as depicted in Figure 5a.

To prove once more that the photons emitted were effectively due to fluorescence, a larger area was visualized, uncovering the bleaching effect caused by the prolonged scanning of the exciting laser beam (Figure 7).

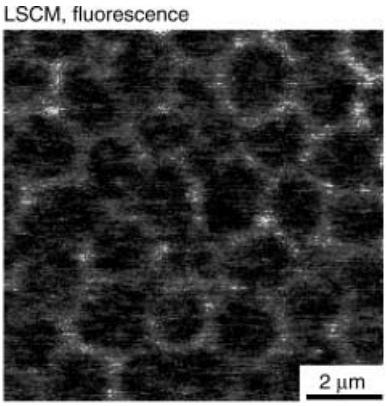

Figure 6. LCSM fluorescence image of a sample bearing nanoparticles with honeycomb-like arrangement covered with a monolayer of dye **3**.

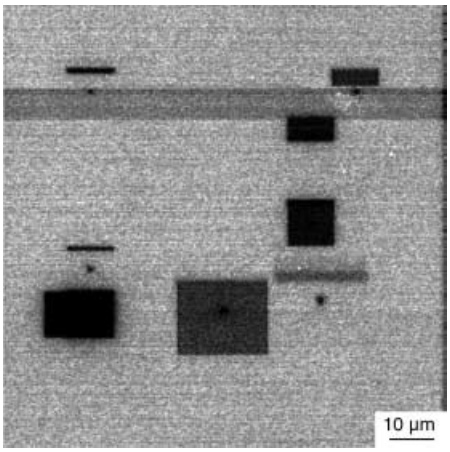

Figure 7. Lower magnification of sample in Figure 6. The dark squares correspond to areas where the fluorophore was bleached by the scanning laser.

When a sample with bare Au was imaged by LSCM for comparison, no fluorescent signal nor the hexagonal pattern could be monitored, demonstrating indeed that scattering and Raman effects could be neglected.

As a final experiment, a second type of sample was prepared. The cavities formed by the condensation pattern were completely filled with micelles by spin-coating with an $AuCl_4^-$-loaded micelle solution of a higher concentration. After plasma etching the substrate was decorated by gold nanoparticles arranged in circular areas (Figure 8). The confocal micrograph in Figure 9a shows that fluorescence is observed in the areas covered by the gold particles. At lower magnification the same sample displays the bleaching effect of the laser on previous scans (Figure 9b) proving that the light emitted from the sample is in fact due to fluorescence.

Conclusion

In summary, we have shown that chemisorption of a fluorescent dye to nanometer-sized gold particles does not fully quench the fluorescence and a recovery of the emitted light is observed. The approach described in this article allows the two-dimensional organization of nanometer-size gold

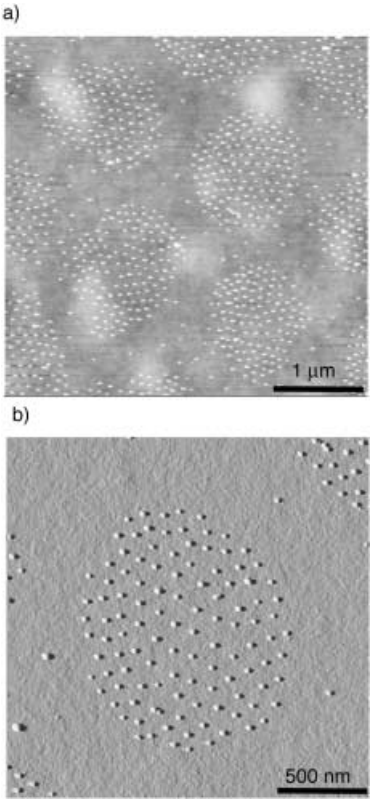

Figure 8. a) and b) Tapping mode AFM height image of filled breath figures at two different magnifications. The micelles uniformly cover the bottom of the breath figure template and are subsequently reduced to nanoparticles by plasma treatment.

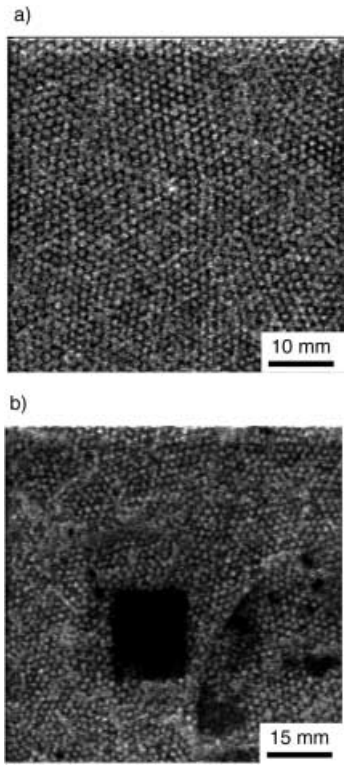

Figure 9. a) Honeycomb morphology of fluorescence on nanostructured substrates. b) The darker spots visible on the image and the dark rectangle show bleaching of adsorbed molecules due to previous scans.

particles on solid supports exploiting capillary forces on prestructured templates. Standard optical techniques can be used and no modified geometries in the setup are needed to detect fluorescence of dyes adsorbed on such structures. We see this approach as a valuable tool for the development of new concepts for HDDS devices and highly sensitive bioanalytical methods.

Experimental Section

Melting points: Melting points were determined with a Reichert melting-point apparatus and are uncorrected.

Chromatographic separations: Chromatographic separations were performed on silica gel 60 (Merck, 0.040–0.063 mm, 230–240 mesh). ^{1}H and ^{13}C spectra were recorded in $CDCl_3$ on a Varian Inova NMR spectrometer, operating at 300 and 75.5 MHz for ^{1}H and ^{13}C, respectively. Chemical shifts are given in ppm relative to tetramethylsilane (TMS). Fast atom bombardment mass spectra (FAB-MS) were measured on a Finnigan MAT 90 spectrometer with *m*-nitrobenzyl alcohol (NBA) as a matrix. **Fluorescence spectra**: Fluorescence spectra in solution were recorded on a SLM-AMINCO SPF-500™ Spectrofluorometer with NOZON®.

Scanning force microscopy (SFM): SFM investigations were performed with a Nanoscope III (Digital Instruments, Santa Barbara, California, USA) operating in the tapping or contact mode. The oscillation frequency for the tapping mode was set in the window 320–360 kHz depending on the Si cantilever ($k \sim 50\ N\,m^{-1}$, Nanosensors). Si_3N_4 cantilevers ($k \sim 0.06\ N\,m^{-1}$, Nanosensors) were used for contact mode imaging.

Laser scanning confocal microscopy: Fluorescence microscopy images were recorded with a α-SNOM (Witech GmbH, Germany) configured with an APD photon counter (EG&G Canada) type SPCM-ARQ-14-FC. The excitation source used was a Ne-YAG laser at 532 nm. A Super-Notch and an interference filter were used to isolate the fluorescence emission from the excitation wavelength. Light was coupled to the microscope with a 50 μm multimode optical fiber. Two different lenses were used: a Plan-Neofluor 63× with 1.25 NA, ∞/0.7 corrected oil immersion lens and an Olympus LCPLAN FL 60×, 0.7 NA air lens. All images were recorded at room temperature, by using excitation laser powers ranging from 30 to 150 μW.

Transmission electron microscopy (TEM): Micrographs were recorded with a CM200 FEG (charge separartion correction).[38] The samples were prepared by casting a solution directly on a carbon-coated copper grid. Excess solution was removed by a soaking tissue so that only a very thin liquid film remained to evaporate.

Materials: All chemicals were purchased by Aldrich and Molecular Probes and purified according to laboratory procedures.[39] Rhodamine B *p*-sulfonyl chloride was isolated from the *ortho*/*para* isomers mixture (Molecular Probes, Oregon USA) by column chromatography (Silica 60 mesh, CH_2Cl_2/CH_3OH, 9:1). High-purity solvents were purchased by Merck and used as received, unless otherwise stated. Syntheses were carried out under argon atmosphere. Tetrachloroauric acid (Fluka, purum), palladium acetate [$Pd(OAc)_2$] (Degussa), and potassium trichloroethylene platinate(II) (Aldrich) were used as received. Toluene (Merck, p.A.) was freshly distilled over sodium/benzophenone, tetrahydrofuran (THF) (Merck, p.A.) from potassium. Blockcopolymers were obtained as described before.[40, 41] The diblock copolymer used here, PS_{1700}-*block*-$P2VP_{450}$, had a polystyrene block of 1700 units linked to a block of 450 2-vinylpyridine units with a polydispersity of $M_w/M_n = 1.13$. Anhydrous hydrazine was prepared by thermolysis of hydrazine cyanurate on a high-vacuum line according to literature procedures.[42] The temperature was raised to 200 °C and the evolving hydrazine was distilled into an ampule, equipped with a poly(tetrafluoroethylene) (PTFE) valve, and stored in the nitrogen-filled glove box before use.

Synthesis of 1-(11-undecyldecylthio)amine 2: Compound **2** was prepared via the phthalimide derivative, starting from 1-(11-undecyldecylthio)bromide previously prepared in our group.[43]

Synthesis of lissamine sulfide 1: Lissamine *p*-Rhodamine B sulfonyl chloride (0.250 g, 0.43 mmol) and 1-(11-undecyldecylthio)amine (148 mg,

  0947-6539/02/0816-3812 $ 20.00+.50/0 *Chem. Eur. J.* **2002**, *8*, No. 16

0.43 mmol) were dissolved in dry CH_2Cl_2 (100 mL). Subsequently triethylamine (1 mL) was added. The reaction mixture was then stirred overnight at room temperature. After cooling the solvent was evaporated under reduced pressure and redissolved in dichloromethane, washed with HCl (1N, 300 mL), 1N $NaHCO_3$ (1N, 300 mL) and brine (300 mL), respectively. Purification by chromatography column (Silica gel, 60 mesh, CH_2Cl_2/MeOH 9:1) gave a dark pink solid (285 mg, 74.9%). M.p. 142–143 °C; ^{1}H NMR (300 MHz $CDCl_3$): $\delta = 8.55$ (d, ^4J(H,H) = 1.5 Hz, 1H; ArCH), 7.85–7.88 (dd, ^3J(H,H) = 7.8 Hz, ^4J(H,H) = 1.5 Hz, 1H; ArC*H*), 7.17 (s, 1H; ArH), 7.15 (d, ^4J(H,H) = 2.4 Hz, 1H; Ar*H*), 6.74–6.78 (dd, ^3J(H,H) = 9.3 Hz, ^4J(H,H) = 2.7 Hz, 2H; Ar*H*), 6.65 (d, ^4J(H,H) = 2.7 Hz, 2H; Ar*H*), 3.55 (q, ^3J(H,H) = 7.2 Hz, 8H; CH_3CH_2N), 2.97 (t, ^3J(H,H) = 7.2, 2H; CH_2NH), 2.50 (t, ^3J(H,H) = 7.3 Hz, 4H; CH_2S), 1.58 (br s, 8H; CH_2CH_2S), 1.15–1.2 (m, 32H; CH_2), 0.9 ppm (t, ^3J(H,H) = 6.8 Hz, 3H; CH_3); ^{13}C NMR ($CDCl_3$) δ = 112.0, 95.2, 76.2–78.0, 47.8–48.5, 45.5, 28.1–28.3, 22.0, 13.5, 12.0 ppm; UV/VIS (CH_2Cl_2): λ_{max} (ε) = 520 nm (88000 $cm^{-1}M^{-1}$); Fluorescence: $\lambda_{exc\ max}$ = 558 nm; $\lambda_{em\ max}$ = 580 nm; FAB-MS: *m/z* calcd [M^+] for $C_{48}H_{73}O_6S_3N_3$: 884.3; found: 884.4; elemental analysis calcd (%) for: $C_{48}H_{73}O_6S_3N_3$: C 65.20, H 8.32, N 4.75, S 10.88; found: C 63.88, H 8.40, N 4.50, S 10.70.

Loading of micelles with metal precursors:[44] A 0.5 wt% solution (c = 5 mg mL^{-1}) of the diblock copolymer PS_{1700}-*block*-$P2VP_{450}$ in dry toluene (V = 5 mL) was stirred for 5 h. L molar equivalents of the metal precursor [$HAuCl_4$] per pyridine unit (L = 0.1–0.5) were added and stirred for at least 24 h. Under vigorous stirring, the micellar solution (2 mL) was quickly added to a 0.02 vol% solution of anhydrous hydrazine in toluene (5 mL). The excess hydrazine (15%) was neutralized with hydrochloric acid directly after reduction and the hydrazinium chloride precipitated.

Preparation of Au-dot-decorated substrates: Glass substrates were covered with gold nanoparticles following a procedure published elsewhere.[15] Glass substrates with thickness of 170 μm (Berliner Glas KG, Robax-Glas AF 45), were cut to 10 × 10 mm^2 pieces, immersed into piraña solution at 70 °C for 15 minutes, extensively rinsed with Milli-Q water (> 15 MΩ), and dried under a nitrogen stream before use. Si wafers (CrysTec, Berlin) were cleaned in piraña as described above. The substrates were fixed on a substrate holder, dipped into the micellar solution (c = 5 mg mL^{-1}) with a velocity of v = 40 mm min^{-1}, and retracted from the solution with a speed of 10 mm min^{-1}. The obtained samples were left to dry upon exposure to air. The substrates coated with a monomicellar film were treated with an oxygen plasma by using a P300 (Plasma Electronics) plasma etcher with a high-frequency generator (Dressler RF-generator LPG 133c). Substrates were treated for 10 min at 120 W. The gas pressure was set at 1 mbar, and the temperature inside the chamber did not exceed 100 °C.

Preparation of breath figures: Preparation of the vitrified condensation patterns has been described before and will be published in further detail elsewhere.[36, 37]

General procedure for the preparation of self-assembled monolayers on gold: All glassware used for monolayer preparation was immersed in piraña solution (66% H_2SO_4 and 33% conc. H_2O_2) at 70 °C for 30 minutes. ***Piraña is a highly oxidative reagent and should therefore be handled with caution.***[45–47] Subsequently, the glassware was rinsed extensively with large amounts of highly pure water (Milli-Q). Before use, the substrates were cleaned in oxygen plasma (120 W, 20 min, 2 mbar) and immersed for 10 minutes in pure ethanol.[48] Substrates were then immerged with minimal delay into a 1 mM solution of **1** in ethanol. Monolayers were prepared at 60 °C.[49] After cooling to room temperature, the substrates were removed from the solution and extensively rinsed with analytical $CHCl_3$, EtOH, and high purity water.

Acknowledgement

Wolfram Ibach, Manuel Rodriguez Goncalves (Experimental Physics, University of Ulm), and Olaf Hollricher (Witech GmbH, Germany) are gratefully acknowledged for the support in the laser scanning fluorescence microscopy measurements and for their interest shown in our research. Silke Riethmüller, (Macromolecular and Organic Chemistry III, University of Ulm) is gratefully acknowledged for the preparation of the shadow-mask gold-evaporated samples. The authors thank for financial support "Deutsche Forschungsgemeinschaft, SFB 569, Teilprojekt G2" and the Nanolink Project of the University of Twente and MESA+ Research Institute, University of Twente.

[1] S. Shinada, F. Koyama, K. Suzuki, K. Goto, K. Iga, *Opt. Rev.* **1999**, *6*, 486–488.
[2] S. Cowen, *Chem. Ind.* **1999**, 584–586.
[3] J. W. Attridge, P. B. Daniels, J. K. Deacon, G. A. Robinson, G. P. Davidson, *Biosens. Bioelectron.* **1991**, *6*, 201–214.
[4] C. Nistor, J. Emneus, *Waste Manage.* **1999**, *19*, 147–170.
[5] K. Sokolov, G. Chumanov, T. M. Cotton, *Anal. Chem.* **1998**, *70*, 3898–3905.
[6] S. Weiss, *Science* **1999**, *283*, 1676–1683.
[7] S. Chu, *Science* **1991**, *253*, 861–866.
[8] T. T. Perkins, S. R. Quake, D. E. Smith, S. Chu, *Science* **1994**, *264*, 822–826.
[9] R. E. Betzig, J. K. Trautman, R. Wolfe, E. M. Gyorgy, P. L. Finn, M. H. Kryder, C. H. Chang, *J. Appl. Phys.* **1993**, *73*, 5791–5798.
[10] A. N. Shipway, E. Katz, I. Willner, *ChemPhysChem* **2000**, *1*, 18–52.
[11] S. Brasselet, W. Moerner, *Single Mol.* **2000**, *1*, 17–23.
[12] I. Willner, R. Blonder, A. Dagan, *J. Am. Chem. Soc.* **1994**, *116*, 3121–3122.
[13] I. Willner, S. Rubin, R. Shatzmiller, T. Zor, *J. Am. Chem. Soc.* **1993**, *115*, 8690–8694.
[14] A. Doron, E. Katz, M. Portnoy, I. Willner, *Angew. Chem.* **1996**, *108*, 1626–1628; *Angew. Chem. Int. Ed. Engl.* **1996**, *35*, 1535–1537.
[15] J. P. Spatz, S. Mössmer, C. Hartmann, M. Möller, T. Herzog, M. Krieger, H. G. Boyen, P. Ziemann, B. Kabius, *Langmuir* **2000**, *16*, 407–415.
[16] J. Brugger, J. W. Berenschot, S. Kuiper, W. Nijdam, B. Otter, M. Elwenspoek, *Microelectron. Eng.* **2000**, *53*, 403–405.
[17] J. Kummerlen, A. Leitner, H. Brunner, F. R. Aussenegg, A. Wokaun, *Mol. Phys.* **1993**, *80*, 1031–1046.
[18] K. H. Drexhage, *Ber. Bunsen-Ges.* **1968**, *72*, 329–345.
[19] J. Enderlein, *Chem. Phys.* **1999**, *247*, 1–9.
[20] S. Reese, M. A. Fox, *J. Phys. Chem. B* **1998**, *102*, 9820–9824.
[21] C. Sönnichsen, S. Geier, N. E. Hecker, G. von Plessen, J. Feldmann, H. Ditlbacher, B. Lamprecht, J. R. Krenn, F. R. Aussenegg, V. Z. H. Chan, J. P. Spatz, M. Möller, *Appl. Phys. Lett.* **2000**, *77*, 2949–2951.
[22] F. R. Aussenegg, A. Leitner, Z. S. Zhao, *Sens. Actuators B* **1994**, *17*, 171–174.
[23] G. Chumanov, K. Sokolov, B. W. Gregory, T. M. Cotton, *J. Phys. Chem. A* **1995**, *99*, 9466–9471.
[24] F. R. Aussenegg, A. Leitner, M. E. Lippitsch, *Rev. Roum. Phys. B* **1988**, *33*, 349–352.
[25] H. Hovel, S. Fritz, A. Hilger, U. Kreibig, M. Vollmer, *Phys. Rev. B* **1993**, *48*, 18178–18188.
[26] U. Kreibig, M. Vollmer, *Optical Properties of Metal Clusters*, Springer, Berlin, **1995**.
[27] R. Chance, A. Prock, R. Silbey, *Adv. Chem. Phys.* **1978**, *37*, 1–65.
[28] G. A. Robinson, *Biosens. Bioelectron.* **1991**, *6*, 183–191.
[29] L. J. Kricka, *Clin. Chem.* **1994**, *40*, 347–357.
[30] R. L. Birke, J. R. Lombardi, R. J. Gale, *Spectroelectrochemistry: Theory and Practice*, Plenum, New York, **1988**.
[31] R. R. Ernst, G. Bodenhausen, A. Wokaun, *Principles of Nuclear Magnetic Resonance in One and Two Dimensions*, Oxford University Press, **1987**.
[32] J. C. Rubim, J. H. Kim, E. Henderson, T. M. Cotton, *Appl. Spectrosc.* **1993**, *47*, 80–84.
[33] Adding metal precursor like $HAuCl_4$, H_2PtCl6, $InCl_2$, $FeCl_3$, $Pd(OAc)_2$, $Ag(OAc)$, $AgNO_3$, $TiCl_4$, $CoCl_2$, and GaH_3 to a micellar solution of PS-*block*-P2VP in toluene and stirring the solution for 12 hours allows the uniform dispersion of the metal precursor over all micelles. After approximately 24 hours each micelle contains the same amount of metal being complexed to the P2VP blocks.
[34] M. Möller, J. P. Spatz, S. Moessmer, P. Eibeck, P. Ziemann, *Abstr. Pap. Am. Chem. Soc.* **1999**, *217*, 003.
[35] J. A. Massey, M. A. Winnik, I. Manners, V. Z. H. Chan, J. M. Ostermann, R. Enchelmaier, J. P. Spatz, M. Möller, *J. Am. Chem. Soc.* **2001**, *123*, 3147–3148.

  0947-6539/02/0816-3813 $ 20.00+.50/0

[36] A. Mourran, S. S. Sheiko, M. Krupers, M. Möller, *PMSE Proc. Am. Chem. Soc.* **1999**, *80*, 185 – 186.
[37] A. Mourran, S. S. Sheiko, M. Möller, *PMSE Proc. Am. Chem. Soc.* **1999**, *81*, 426 – 427.
[38] M. Haider, H. Rose, S. Uhlemann, E. Schwan, B. Kabius, K. Urban, *Ultramicroscopy* **1998**, *75*, 53 – 60.
[39] D. D. Perrin, W. F. L. Amarego, *Purification of Laboratory Chemicals*, Pergamon, Oxford, **1989**.
[40] J. P. Spatz, S. Sheiko, M. Möller, *Macromolecules* **1996**, *29*, 3220 – 3226.
[41] S. Mössmer, J. P. Spatz, M. Möller, T. Aberle, J. Schmidt, W. Burchard, *Macromolecules* **2000**, *33*, 4791 – 4798.
[42] E. Nachbaur and G. Leiseder, *Monatsh. Chem.* **1971**, *102*, 1718 – 1722.
[43] M. W. J. Beulen, F. C. J. M. van Veggel, D. N. Reinhoudt, *Chem. Commun.* **1999**, 503 – 504.
[44] J. P. Spatz, S. Mössmer, M. Möller, *Chem. Eur. J.* **1996**, *2*, 1552 – 1555.
[45] D. A. Dobbs, R. G. Bergman, K. H. Theopold, *Chem. Eng. News* **1990**, *68*, 22.
[46] T. Wnuk, *Chem. Eng. News* **1990**, *68*, 22.
[47] S. L. Matlow, *Chem. Eng. News* **1990**, *68*, 22.
[48] H. Ron, I. Rubinstein, *Langmuir* **1994**,*10*, 4566 – 4573.
[49] Previously we have shown that for sulfide monolayers an elevated adsorption temperature of 60 °C increases the quality of the monolayer: a) B. H. Huisman, E. U. Thoden van Velzen, F. C. J. M. van Veggel, J. F. J. Engbersen, D. N. Reinhoudt, *Tetrahedron Lett.* **1995**, *36*, 3273 – 3276; b) E. U. Thoden van Velzen, J. F. J. Engbersen, P. J. Delange, J. W. G. Mahy, D. N. Reinhoudt, *J. Am. Chem. Soc.* **1995**, *117*, 6853 – 6862; c) B. H. Huisman, D. M. Rudkevich, F. C. J. M. van Veggel, D. N. Reinhoudt, *J. Am. Chem. Soc.* **1996**, *118*, 3523 – 3524.

Received: January 17, 2002 [F3806]

  0947-6539/02/0816-3814 $ 20.00+.50/0